Vol. 333: 161–171, 2007 | MARINE ECOLOGY PROGRESS SERIES
Mar Ecol Prog Ser | Published March 12

Effects of spatangoid heart urchins on O_2 supply into coastal sediment

Kay Vopel[1,*], Angelika Vopel[2], David Thistle[3], Nicole Hancock[1]

[1]National Institute of Water and Atmospheric Research, PO Box 11115, Hamilton, New Zealand
[2]202 Mandeno Street, Te Awamutu 3800, New Zealand
[3]Department of Oceanography, Florida State University, Tallahassee, Florida 32306–4320, USA

ABSTRACT: Spatangoid heart urchins are key bioturbators in the marine environment. They pump seawater from the sediment surface around their tests and, at the same time, constantly displace the surrounding sediment. To improve our understanding of the effects of this activity on the oxygenation of coastal sediment, we studied for the first time *in situ* [O_2] around *Echinocardium cordatum* at sub-millimeter resolution under different hydraulic conditions. In the laboratory, we investigated the effects of *E. cordatum* on pore-water pH and sediment apparent diffusivity. Individuals advancing 1 to 3 cm h^{-1} through the upper 4 cm of the sediment displaced a greater volume of seawater than sediment per unit time. The O_2 uptake of the sediment surrounding *E. cordatum* was at least twice the respiration of the echinoids. Besides creating additional sediment contact with oxygenated seawater, *E. cordatum* affected the supply of O_2 to the sediment by altering photosynthetic O_2 production at the sediment surface, and increasing the exchange area of the sediment–seawater interface and apparent diffusivity of the uppermost sediment layer. After the passage of an individual, pore-water [O_2] profiles indicative of benthic photosynthesis recovered rapidly from the disturbance, but the pH of deeper pore water was altered. *In situ*, time series measurements of [O_2] and hydrostatic pressure indicated that wind waves can increase the transport of O_2 across both the sediment–seawater interface and the interface between the seawater surrounding *E. cordatum* and the adjacent sediment.

KEY WORDS: Bioturbation · Bioirrigation · Microphytobenthos · Benthic photosynthesis · Diffusion · Advection · Waves · Dissolved oxygen · Apparent diffusivity

INTRODUCTION

The pathways and rates of O_2 supply to marine sediment are of interest because O_2 plays a key role in early diagenetic reactions, in particular the mineralization of organic matter. In the shallow subtidal, enough light reaches the seabed that benthic algae and cyanobacteria on or very near the sediment surface photosynthesize, and their production of O_2 has a dominating effect (Fenchel & Glud 2000). In the absence of large bioturbating animals, the O_2 that these phototrophs produce may pass into the overlying seawater and the pore water of deeper sediment by both diffusion and advection. Although these processes and their effects are relatively well known, the role of bioturbators is complex and not well understood.

In shallow-subtidal areas, burrowing heart urchins (Echinoidea: Spatangoida) appear to be important bioturbators because they are large and common (Osinga et al. 1995, Bird et al. 1999, Hollertz & Duchêne 2001). While moving horizontally through the sediment, these echinoids both pump oxygenated seawater from the sediment surface toward and around their outer surfaces (irrigation), and displace particles and pore water of the surrounding sediment (Buchanan 1966, De Ridder et al. 1987, Kanazawa 1995). Heart urchins mainly affect the sediment oxygenation by creating additional sediment–seawater contact beneath the visible sedi-

*Email: k.vopel@niwa.co.nz

ment surface; furthermore, at some locations, they rework the sediment at depth where their passage also affects the visible sediment surface and the phototrophic organisms living there (Lohrer et al. 2004). These 2 interactions combined may modify the O_2 supply to the sediment, but mechanistic understanding of them is inadequate.

Here we report the effects of a burrowing heart urchin on the oxygenation of shallow-subtidal sediment. We asked whether its activity can affect production, consumption, and transport of O_2 at the sediment–seawater interface. The effect of heart urchins on these processes may vary according to the rates at which they irrigate and displace sediment. To estimate these rates, we measured the heart urchin's speed of locomotion, its respiration, the oxygenation of its respiratory current, and the O_2 uptake of surrounding sediment. Because we expected irrigation and displacement of sediment by heart urchins to change the relative importance and depth distribution of benthic reduction-oxidation reactions and, therefore, the production and consumption of protons, we studied pore-water pH. Finally, we asked whether particle reworking by heart urchins can affect the diffusivity of the uppermost sediment. We chose to study the spatangoid *Echinocardium cordatum* (Pennant, 1777) because its large size, rapid movement rate, high local abundance, and broad regional distribution made it interesting both as a model of bioturbation and as a bioturbator in its own right. Because the solute-transport regime at the sediment surface (which influences pore-water oxygenation) is sensitive to changes in the characteristics of the near-bottom flow (Huettel & Webster 2000), we conducted some of our measurements under different hydraulic conditions.

MATERIALS AND METHODS

Locality, sediment properties, and echinoid behavior. The study site was on unvegetated sediment at 4 to 5 m depth at the mouth of Mahurangi Harbour (36° 30.74′ S, 174° 43.55′ E) on the eastern shore of the North Island, New Zealand. Mahurangi Harbour is a small estuary (about 25 km^2) that is sheltered from ocean swell. Because freshwater input is low, the harbour is almost isohaline (salinity > 33), and circulation in the estuary is driven primarily by the tide. Neap and spring tidal ranges are 1.4 and 3.1 m, respectively. The average porosity (ϕ) of the upper 3 cm of sediment was 0.40 (SD = 0.015, n = 6), determined as the weight loss of a known volume of sediment after drying at 105°C for 48 h. The organic content of the sediment was 2.7 % (dry wt), measured as weight loss when the sediment was dried at 105°C for 48 h and then combusted at 400°C for 6 h. The inclusive sorting coefficient of the sediment was 0.93, and the median grain size was 191 (SD = 5 µm, n = 6; see Giere [1993] for details on granulometric measures). On the Wentworth scale, the sediment was a moderately sorted, fine sand.

As *Echinocardium cordatum* moves, it leaves a sediment depression along its path that is flanked by ridges; this combination we term its track (Fig. 1a). For most burrowing individuals, the tips of the enlarged primary spines of the interabulacral plates of the frontal groove and apex extend to the surface of the sediment (Fig. 1b). The primary spines of the frontal groove create a large funnel (front funnel, Fig. 1b) that connects the sediment surface with the adapical and fasciolar region of the frontal groove. The apical tuft of spines forms a backwards-oriented, tapered funnel (rear funnel, Fig. 1b,c), which opens flush with the sediment surface. This tuft creates a ~2 mm diameter aperture by which seawater is admitted to the surface of the test (Nichols 1959). The opening of the rear funnel is higher than the opening of the front funnel. Individuals of *E. cordatum* that are not moving maintain several conduits < 2 mm diameter rather than a large front funnel.

Abundance, speed of movement, and test and track dimensions. To estimate the abundance of *Echinocardium cordatum,* a SCUBA diver counted all individuals in 16 randomly placed, 50 × 50 cm quadrats by systematically pulling his fingers through the upper 10 cm of the seabed. To estimate the speed with which *E. cordatum* moved through the sediment, he marked the position of the rear funnel (Fig. 1b) and measured the distance between this marker and the new position of the funnel after 30 min. To measure distance moved, he photographed a ruler on the surface of the sediment, the marker, and the opening of the rear funnel using a Sony Cyber-shot DSCP-8 digital camera in an underwater housing.

To estimate the depth and width of a track, the diver photographed a ruler that had been pushed vertically into the sediment normal to the center line of the track (Fig. 1a). We defined the track width as the horizontal distance between the outer edges of the ridges. The vertical distance between the highest point of the ridge and the bottom of the depression was defined as the track depth. To measure the length, width, and height of the echinoids with and without spines, we took digital photographs of specimens with a ruler in the field of view. We calibrated the images by means of the scale on the ruler, and we measured all distances using image-analysis software.

In situ* measurements. *Flow speed, hydrostatic pressure, [O_2], and E_d(PAR): We made our field measurements on 3 days in March and April 2004 that had different hydraulic conditions. We determined flow speed either by visually tracking the movement of neutrally

buoyant particles 5 cm above the sediment surface (on 19 March), or by measuring it with a Nortek acoustic-Doppler velocimeter (ADV, on 13 and 14 April) that was also equipped with a pressure sensor. Because pore-water [O_2] at our study site was likely to have been affected by benthic photosynthesis, we measured the incident downwelling irradiance of photosynthetically active radiation (hereafter E_d(PAR); PAR = wave lengths between 400 and 700 nm) at the sediment surface using a plane underwater quantum sensor (LI-192SA, LI-COR Environmental). [O_2] in sediment pore water or near-bottom seawater was measured with a Clark-type microelectrode with internal reference and guard cathode (Revsbech 1989) and a picoammeter (PA3000U, Unisense). The O_2 microelectrode had an outside tip diameter of ~50 µm, and a 90% response time of <1 s. The stirring sensitivity was <2%, and the detection limit was 0.3 µmol l^{-1}. On 13 and 14 April, in order to record synchronous time series of flow velocity, hydrostatic pressure, [O_2], and E_d(PAR), we mounted the ADV and underwater quantum sensor on a rack that was then placed on the sediment surface by SCUBA divers. The center line of the ADV was parallel to the sediment surface at 40 cm above the sediment. The head of the underwater quantum sensor was 2 cm above the sediment surface, facing upward. A SCUBA diver attached the O_2 microelectrode to a manually operated micromanipulator (Märzhäuser Wetzlar) mounted on an aluminum post that had been driven into the sediment. Depending on the data required, he subsequently positioned the microelectrode to measure the [O_2] in the near-bottom seawater, in the pore water of the sediment at a depth of 0.5 or 10 mm, or in the intrafasciolar region of a burrowing *Echinocardium cordatum*. The ADV, quantum sensor, and picoammeter were connected to recorders at the surface through independent cables. The internal data logger of the ADV logged the signals of the sensors for velocity and [O_2] at 16 Hz. Simultaneously, a LI-1000 data logger (LI-COR Environmental) recorded averages of E_d(PAR) every minute (sampling interval = 1 s). In addition, we recorded the salinity and pH of the seawater 50 cm below its surface every 30 min with 2 PortaMess 913 meters, one using a conductivity sensor (SE 204) and the other a pH sensor (Pt1000 electrode SE 102, Knick).

Pore-water [O_2] microprofiles: On 19 March, we measured vertical [O_2] profiles in the centers of the tracks of 4 randomly selected, moving *Echinocardium cordatum* (~1.5 cm behind the echinoid) and in adjacent (15 to 20 cm distant), undisturbed sediment. We then measured an [O_2] profile in the sediment above each echinoid between the openings of the front and rear funnels (indicated by the asterisk in Fig. 1b). To make a profile, a SCUBA diver moved the O_2 microelectrode in 100 µm increments normal to the sediment surface from a position above the diffusive boundary layer to a maximal sediment depth of 10 mm. The SCUBA diver was 40 cm away from the electrode, and his body center line was normal to the main direction of the near-bottom seawater flow. When the sensor was in position, he recorded the value, which was stable. The discontinuity of the concentration gradient was used as the indicator of the interface between the respiratory current of *E. cordatum* and the sediment.

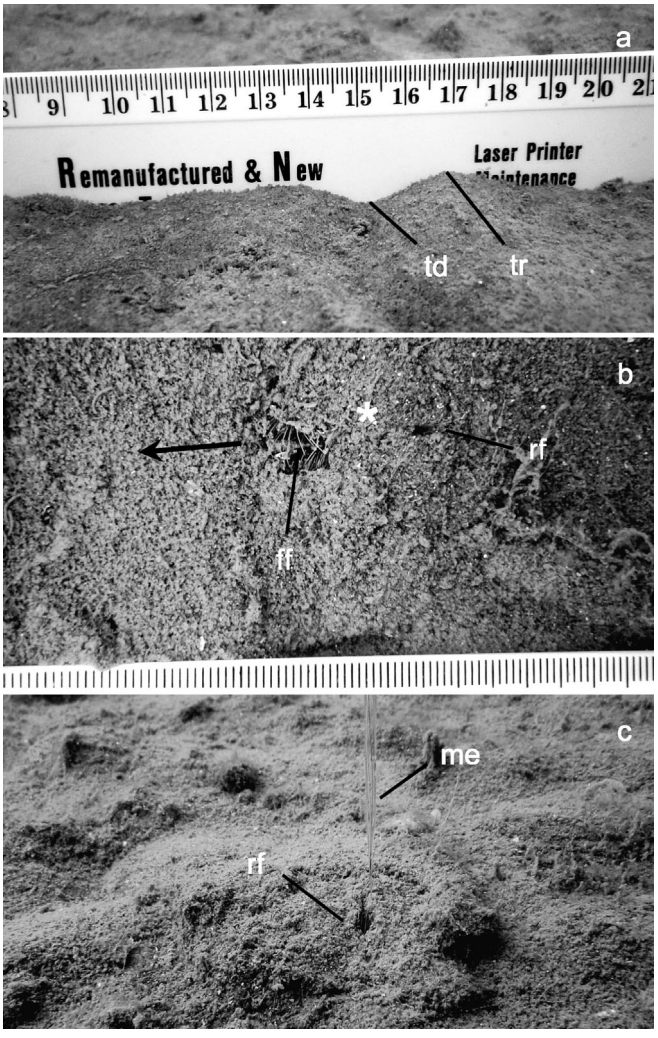

Fig. 1. *Echinocardium cordatum*. Underwater photographs of sediment surface: (a) cross section of a track, (b) plan view of the sediment above a buried echinoid, including the opening of rear and front funnels, and (c) Clark-type microelectrode measuring [O_2] at the rear funnel opening. ff: front funnel; me: microelectrode; td: track depression; tr: track ridge; rf: rear funnel. Arrow indicates the direction of movement of the echinoid; the ruler is marked in mm and cm; * indicates the position between the aboral and front openings at which the sediment above the echinoid was penetrated by the microelectrode to measure vertical profiles of porewater [O_2]

Laboratory measurements. ***Establishment of aquaria:*** To measure sediment profiles of [O_2], pH, and apparent diffusivity (the product of the sediment porosity, ϕ, and the effective diffusion coefficient, D_S), we set up 3 rectangular aquaria (44 cm long, 17 cm deep, 26 cm wide) in a constant-temperature laboratory (15°C). To obtain sediment for the aquaria, SCUBA divers collected 9 cores with hand-held, plastic tubes (10 cm diameter, 20 cm long) that could be closed at both ends. We used a sieve of 0.5 mm aperture to remove large particles (e.g. shell fragments) and macrobenthic animals. Thereafter, we collected 45 individuals of *Echinocardium cordatum* from the study site and measured their lengths (see below). The sieved sediment and 15 large (>35 mm length) echinoids were then transported to the laboratory. During transit and in the laboratory, the echinoids were kept in a seawater bath at approximately *in situ* temperature. We filled each aquarium with 5 cm of sediment, and after 7 d (for consolidation and establishment of new physico-chemical and biological gradients), we added 5 echinoids (density equivalent to ~53 ind. m^{-2}). The color of the undisturbed sediment surface in the aquaria was mainly greenish-brown, but also grey in places.

A bilge pump (Bilge Mate 32-1015-01, Johnson) pumped seawater from a common, 20 l reservoir through a silicon tube into each aquarium. To dissipate turbulence caused by the in-flowing seawater jet, we inserted a baffle consisting of a plate with 5 mm-diameter holes (23 holes in each of 8 horizontal rows), 6 cm from the upstream end of each aquarium. The seawater traveled through the baffle, over the sediment, and left the aquarium by gravity through a horizontal row of holes along the upper edge of the downstream wall. The seawater depth in the aquaria was ~10 cm. The flow speed in the aquaria, which we measured by tracking neutrally buoyant particles ~5 cm above the sediment surface, was ~2 cm s^{-1}, much less than that needed to erode the sediment. We monitored the temperature, salinity, and pH of the seawater in the aquaria throughout the experiments by the same methods used in the field. The average temperature of the seawater was 14.5 ± 0.2°C, average salinity was 35.1 ± 0.4, and average pH was 8.1 ± 0.1 (mean ± SD, n = 8). E_d(PAR) measured at the surface of the sediment in aquaria was 77 µmol quanta m^{-2} s^{-1}.

Pore water profiles of [O_2], pH, and apparent diffusivity: In each of 3 aquaria, 2 [O_2] profiles and 2 pH profiles were measured in the center of the track of 1 *Echinocardium cordatum* (~1.5 cm behind the echinoid) and in the adjacent, greenish-brown, undisturbed sediment (~20 cm distant from the echinoid). Thereafter, we recorded 1 [O_2] profile in the sediment above 1 *E. cordatum* in each aquarium. Profiles of apparent gas diffusivity were recorded in the center of a track, in the accumulated sediment at the ridge of this track, and in the adjacent undisturbed sediment.

To measure profiles of [O_2], pH, and apparent gas diffusivity in the laboratory, we mounted Unisense microelectrodes on a motorized micromanipulator that was attached to a stand. The software PROFIX (Unisense) controlled the step-wise movement of the micromanipulator by means of a motor controller, and recorded the data from the microsensor amplifiers through an A/D converter (ADC-216USB, Unisense). The tip diameters of the microelectrodes for pH and redox potential were 0.05 mm, and the tip diameter of the apparent gas diffusivity microelectrodes was 0.5 mm. We measured apparent gas diffusivity by monitoring the diffusion of H_2 from an internal reservoir through an internal diffusion barrier in the sensor tip and out into the surrounding pore water of the sediment (for more details see Revsbech et al. 1998).

Respiration, body dimensions, and volume of Echinocardium cordatum: Ten adult specimens of *E. cordatum* were removed from the sediment in the aquaria and rinsed in 0.7 µm-filtered seawater. One individual was transferred to each of ten 100 ml flasks filled with normoxic, 0.7 µm-filtered seawater (pH = 8.1 ± 0.1, T = 15.4 ± 0.4°C, S = 35.2 ± 0.7). No sediment was added. We measured the [O_2] continuously during a 2 h (dark) incubation with a needle-type, fiber-optic microsensor (an optode) and a Microx TX O_2 meter (Precision Sensing). Flasks of filtered seawater served as controls. To measure wet weight, we rinsed each specimen in 0.7 µm-filtered seawater, transferred it to a sieve, and weighed it. For dry weight, each specimen was rinsed with distilled water, dried at 70°C for 24 h, and weighed again. Body volumes were measured by displacement of water. We calculated an individual's respiration rate from the decrease of [O_2] in its flask.

Sensor calibrations. We calibrated the microelectrodes and the optode once a day at the experimental temperature (15°C). The diffusivity microelectrode was calibrated by measurement of the electrode current in 2 media of known diffusivity: 0.04 to 0.06 mm diameter glass beads, and in static seawater. We calculated the reference value for the diffusivity of H_2 in static seawater from the diffusivity of O_2 (Broecker & Peng 1974) corrected for temperature by the method of Li & Gregory (1974). The apparent diffusivity in glass beads was taken from Revsbech et al. (1998). We used commercial buffers to calibrate the pH microelectrode. The O_2 microelectrode and optode were calibrated in 100% air-saturated seawater and in seawater that had been deoxygenated with sodium sulfite.

Data analysis. The depth-integrated, O_2-consumption or -production rate (R) of the sediment was computed from *in situ* [O_2] profiles using the methods of

Berg et al. (1998). We detected the position of the sediment–seawater interface from abrupt changes in the slope of the O_2 profiles (Rasmussen & Jørgensen 1992). The sediment diffusion coefficient for O_2 was calculated from the free-solution diffusion coefficient (D_0) and ϕ according to $D_S = \phi^{(m-1)} \times D_0$, where $m = 3$ (Ullman & Aller 1982). Values for D_0 were taken from Broecker & Peng (1974) and were recalculated to the experimental temperature with the Stokes-Einstein relation (Li & Gregory 1974). We assumed ϕ and D_S to be constant with depth, and we ignored any effects of meiofauna on solute transport. For analyses of time series, we used the software system Statistica (StatSoft). Time series were transformed by simple exponential smoothing (no trend, no season, $\alpha = 0.1$), and the periodogram values were smoothed with a weighted moving average (i.e. a Tukey window). Whenever an indicator of variation is given, it is 1 SD. We used parametric ANOVA to test for statistical significant differences in O_2 penetration depth. Differences in [O_2] maxima and the depth of these maxima were tested with 2-sample *t*-tests ($\alpha = 0.05$).

RESULTS

Abundance, speed of movement, and tracks

In the field, about 70% of the *Echinocardium cordatum* population (abundance = 46.63 ± 16.23 ind. m^{-2}, n = 16) moved through the sediment at a depth of 10.5 ± 5.4 mm (n = 23) and at speeds of ~1 to 3 cm h^{-1}. The remaining individuals (hereafter referred to as stationary) did not move. The average distance between the aboral and frontal openings was 14.7 ± 3.1 mm (n = 61). The color of the sediment surface was grey immediately behind a moving echinoid but was greenish-brown otherwise. Tracks were easily distinguishable from much smaller surface structures produced by, for example, polychaetes and small crustaceans. The average track width was 34.0 ± 6.0 mm (n = 25), and average track depth was 3.8 ± 1.0 mm (n = 25). Echinoids placed in the aquaria immediately started burrowing into the sediment and completed burial after ~2 h. Thereafter, they either moved through the sediment at a depth of 3.6 to 5.0 mm (distance between dorsal surface and sediment surface) or remained stationary 16 to 18 mm below the sediment surface.

Flow velocity, hydrostatic pressure, and E_d(PAR)

During the 3 days of our field measurements, the salinity of the seawater was between 35.2 and 35.3 and the pH between 8.1 and 8.2, but the temperature of the near-bottom seawater decreased from 19.5 to 16.7°C (Table 1).

On 19 March, the weather was calm, the seawater surface was flat, and the flow of the near-bottom seawater was steady (1.5 ± 0.2 cm s^{-1}). Passing clouds episodically decreased E_d(PAR) to as little as 61 µmol quanta m^{-2} s^{-1}. During measurements of [O_2] in the sediment of *Echinocardium cordatum* tracks and in the adjacent, undisturbed sediment (see below), E_d(PAR) varied between 128 and 472 µmol quanta m^{-2} s^{-1} (average 260 ± 125 µmol quanta m^{-2} s^{-1}, Table 2) and between 63 and 267 µmol quanta m^{-2} s^{-1} (average 156 ± 93 µmol quanta m^{-2} s^{-1}), respectively. The average E_d(PAR) during measurements in the sediment above burrowing *E. cordatum* was 263 ± 93 µmol quanta m^{-2} s^{-1} (min. = 72, max. = 379).

On 13 April, the orbital motion of swell reached the surface of the sediment, so that the hydrostatic pressure and horizontal velocity of the near-bottom seawater fluctuated at regular intervals. Spectral analyses of the time series of pressure and velocity revealed peaks in the spectral densities at periods of 11.0 ± 0.4 and 10.9 ± 0.4 s, respectively (n = 5, see Fig. 2a,b for example analyses). E_d(PAR) varied between 26 and 458 µmol quanta m^{-2} s^{-1}.

On 14 April, wind waves approached the mouth of Mahurangi Harbour in addition to swell. The hydrostatic pressure and speed of the horizontal flow fluctuated at 2 regular intervals: the densities of the spectra peaked at periods of 3.4 ± 0.2 and 10.1 ± 0.5 s for hydrostatic pressure, and 3.6 ± 0.1 and 10.0 ± 0.1 s for flow speed (n = 4, example analyses shown in Fig. 2d,e). E_d(PAR) ranged from 25 to 306 µmol quanta m^{-2} s^{-1}.

Table 1. Abiotic parameters (mean ± 1 SD) at the study site at the mouth of Mahurangi Estuary, New Zealand, in 2004. E_d(PAR) is downwelling irradiance of photosynthetically active radiation incident at the sediment surface (µmol quanta m^{-2} s^{-1})

Date	Time (h)	E_d(PAR) Min.	E_d(PAR) Max.	Temp (°C)	Salinity	pH	Flow speed (cm s^{-1}) Min.	Flow speed (cm s^{-1}) Max.
19 March	10:00–15:00	60.8	462.6	19.5 ± 0.2	35.2 ± 0.1	8.2 ± 0.3	1.2	1.7
13 April	12:11–16:15	25.5	457.7	16.9 ± 0.1	35.2 ± 0.2	8.1 ± 0.1	4.0 ± 0.9	6.7 ± 1.0
14 April	10:00–15:00	24.7	306.2	16.7 ± 0.1	35.3 ± 0.2	8.1 ± 0.1	2.8 ± 0.4	7.5 ± 1.0

Table 2. Summary of field (19 March 2004) and laboratory measurements in undisturbed and track sediments, and sediments above *Echinocardium cordatum* (mean ± 1 SD). Undisturbed sediment had no visual evidence of passage of *E. cordatum*. O_2 penetrated sediment above *E. cordatum* from the near-bottom seawater and respiratory current around the echinoid. OPD: O_2 penetration depth; D_m: depth of $[O_2]$ maximum; $[O_2]_m$: maximum $[O_2]$; *R*: depth-integrated O_2-production or -consumption rate computed from the best-fitting $[O_2]$ profile following Berg et al. (1998)

	E_d(PAR) (µmol quanta m^{-2} s^{-1})	OPD (mm)	D_m (mm)	$[O_2]_m$ (% saturation)	R (µmol m^{-2} h^{-1})
In situ **(n = 4)**					
Undisturbed	156 ± 93	3.6 ± 0.5	0.4 ± 0.1	196 ± 67	202
Track	260 ± 125	2.4 ± 0.2	0.2 ± 0.1	132 ± 67	96
Above echinoid					
From near-bottom seawater	263 ± 93	2.0 ± 0.2	–	–	−98 ± 31
From respiratory current		0.5 ± 0.2	–	–	−152 ± 99
Ex situ **(n = 3)**					
Undisturbed	77	4.4 ± 0.4	0.5 ± 0.1	149 ± 10	
Track	77	4.2 ± 0.2	0.5 ± 0.1	124 ± 10	
Above echinoid					
From near-bottom seawater	77	2.0 ± 0.3	–	–	
From respiratory current		0.4 ± 0.3	–	–	

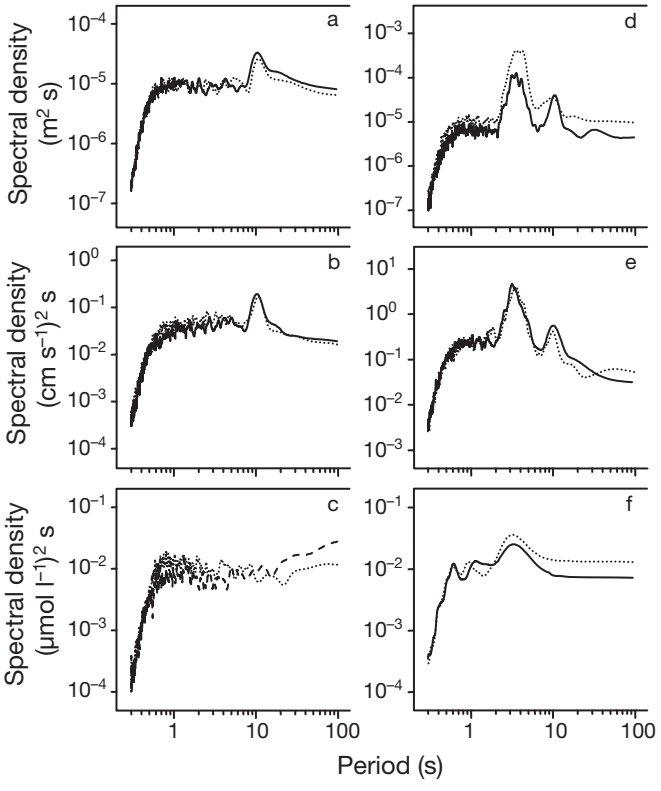

Fig. 2. Spectra of 20 min time series of (a,d) hydrostatic pressure, (b,e) flow speed, and (c,f) $[O_2]$ recorded at the mouth of Mahurangi Estuary, New Zealand, on (a–c) 13 and (d–f) 14 April 2004. Measurements began at 12:40 h (solid line), 13:30 h (dotted line), and 15:20 h (dashed line) on 13 April and at 14:20 h (solid line) and 14:45 h (dotted line) on 14 April. Hydrostatic pressure and flow speed were measured at ~5 m seawater depth, 40 cm above sediment surface; $[O_2]$ was measured in the intrafasciolar region of 2 specimens of *Echinocardium cordatum* (dotted and dashed lines) and upper microphytobenthos layer of the undisturbed sediment at 0.5 mm depth (solid line)

$[O_2]$ gradients

Displacement of sediment by *Echinocardium cordatum* as it moved and fed may have removed the surface community of microphytes and disrupted the $[O_2]$ gradients they produce, but our measurements under conditions of steady, unidirectional flow revealed steep gradients in the track sediment, with $[O_2]$ maxima at 132% of air saturation at a depth of 0.2 mm (Fig. 3, Table 2). O_2 penetrated the track sediment to a depth of 2.4 mm. The pore water of the undisturbed sediment was oxygenated to a greater depth (3.6 mm), and $[O_2]$ peaked at a higher saturation of 196%. Similarly, the depth-integrated, net-O_2 production computed from the average $[O_2]$ profile shown in Fig. 3 was higher in the undisturbed sediment (202 µmol m^{-2} h^{-1}) than in the track sediment (96 µmol m^{-2} h^{-1}). O_2 penetrated the 7.9 ± 0.9 mm-thick sediment layer above burrowing *E. cordatum* from 2 directions: 2.0 mm down from the near-bottom seawater, and 0.5 mm up from the respiratory current around the echinoid (Fig. 4, Table 2). $[O_2]$ did not peak at the sediment surface. Average depth-integrated O_2 consumptions in the surface sediment and in the sediment around the echinoid were −98 and −152 µmol m^{-2} h^{-1}, respectively. Differences between mean O_2 penetration and mean depths of O_2 peaks were statistically significant. Mean $[O_2]$ maxima in undisturbed and track sediment, and mean depth-integrated O_2 consumption in the surface sediment and sediment surrounding the echinoid did not differ significantly.

Time series of $[O_2]$

$[O_2]$ in the intrafasciolar regions was 82.7 ± 4.1% (n = 5) of the saturation of the near-bottom seawater. At the

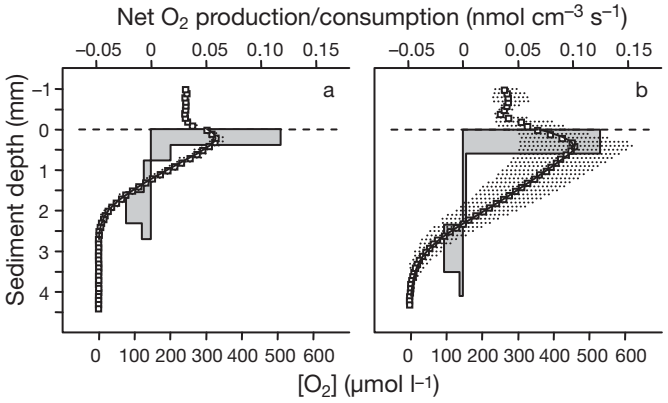

Fig. 3. *In situ* profiles of pore-water [O_2] (□) and net O_2-production/consumption (gray bars) in (a) the center of *Echinocardium cordatum* tracks (1.5 cm behind the echinoid) and (b) undisturbed sediment (15 to 20 cm from nearest echinoid) on 19 March 2004. [O_2] are mean ± 1 SD (n = 4, dotted lines). Profiles of net O_2 production/consumption were calculated from the best-fitting [O_2] profiles. Sediment–seawater interface is located at 0 mm (dashed line). Note: we give [O_2] per volume of pore water, but net O_2 production/consumption per volume of sediment

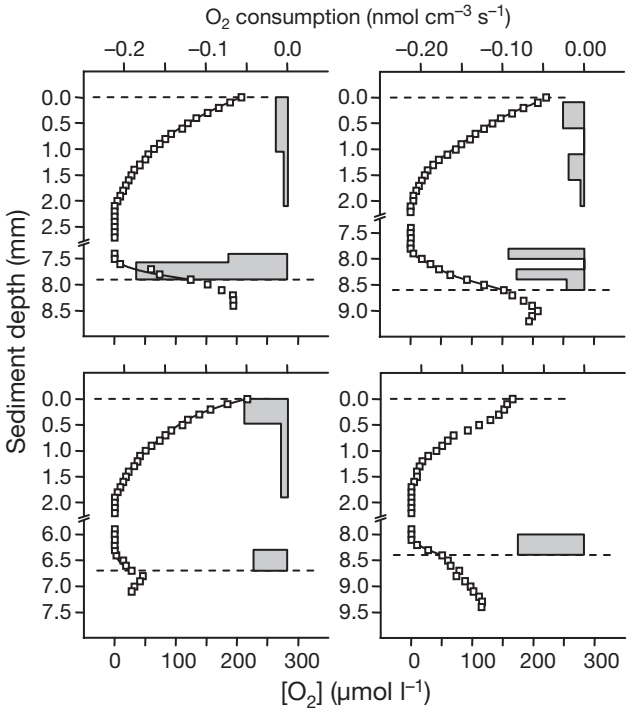

Fig. 4. *In situ* profiles of [O_2] (□) and O_2 consumption gray bars) in the sediment between the front and rear openings of 4 burrowing *Echinocardium cordatum* (asterisk in Fig. 1b). O_2-consumption profiles were calculated from the best-fitting [O_2] profiles. Upper and lower dashed lines indicate positions of the sediment–seawater interface (0 mm) and interface between the seawater surrounding the echinoid and adjacent sediment, respectively. Note break in vertical scale

openings of the rear funnels, [O_2] was ~15% higher than that measured in the intrafasciolar regions, and ~25% higher than that measured at the openings of the front funnels.

Oxygenation of the pore water in the uppermost layer of undisturbed sediment changed rapidly in response to fluctuations in E_d(PAR) owing to the passage of clouds. Such changes were superimposed on diurnal variation caused by changes in the altitude of the sun. Only the latter caused measurable changes in the oxygenation of near-bottom seawater: [O_2] 10 cm above the sediment surface increased during the day to a maximum of 119% air saturation on 13 April and 132% air saturation on 14 April.

Spectral analyses of 20 min time series of [O_2] measured on 14 April under conditions of wind waves with an average period of 3.3 ± 0.1 s (n = 4) revealed cyclic variation in [O_2]. At this time scale, [O_2] varied from 2 to 4% of saturation in the near-bottom seawater and in the pore water of the undisturbed sediment at depths of 0.5 and ~10 mm, and from 10.1 to 14.8% of saturation in the intrafasciolar region of 2 *Echinocardium cordatum* (Fig. 2f). Co-spectrum analyses revealed a correlation between such variations and variations in hydrostatic pressure. The time series on 13 April under wave conditions did not reveal any cyclic variations in [O_2] (see Fig. 2c for example analyses).

Laboratory sediment profiles of [O_2], apparent diffusivity, and pH

The [O_2] profiles measured in aquaria resembled those measured in the field under conditions of steady, unidirectional flow. The sediment (3.6 to 5 mm thick) above burrowing individuals was not fully oxygenated: O_2 penetrated 2.0 mm into the sediment but just 0.4 mm from the interface of the seawater surrounding the echinoid into the adjacent sediment (Table 2). The pore water of the uppermost sediment layers of both the greenish-brown, undisturbed sediments and the tracks were O_2 supersaturated, and average depths of O_2 penetration were similar (Table 2). In both sediments, pH peaked below the sediment surface and then decreased sharply to a minimum at depths of 3 to 5 mm at or just below the oxic–anoxic interface. From 5 to 12 mm depth, pH increased in the track sediment but remained constant in the undisturbed sediment. An example profile is shown in Fig. 5.

The apparent diffusivity of the ridge sediment was higher than that of the undisturbed sediment: average diffusivity calculated from measurements at depths between 2 and 4 mm was 0.76×10^{-5} cm^2 s^{-1} (SD = 0.02×10^{-5}) at the ridge and 0.43×10^{-5} cm^2 s^{-1} (SD = 0.04×10^{-5}) in the undisturbed sediment (Fig. 5). In

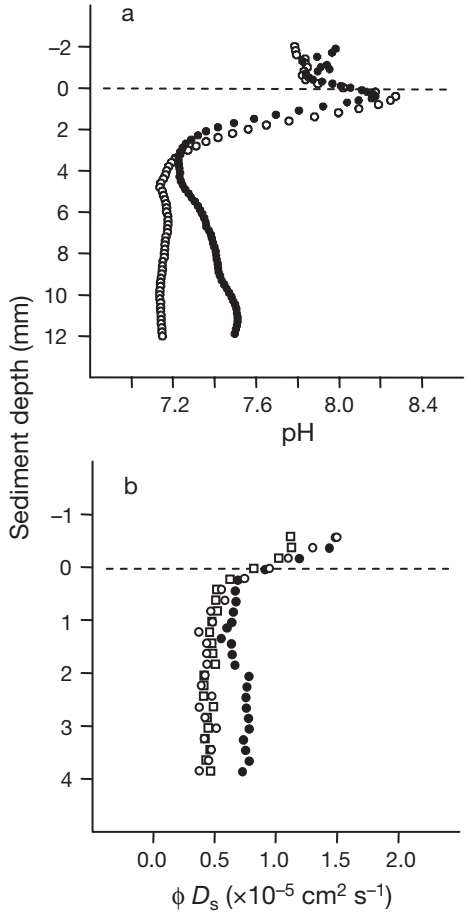

Fig. 5. *Ex situ* profiles of (a) pH and (b) apparent diffusivity ($\phi \times D_S$). pH was measured in undisturbed sediment adjacent to burrowing *Echinocardium cordatum* (○) and 1.5 cm behind an individual in the center of its track (●). Apparent diffusivity was recorded 1.5 cm behind a buried *E. cordatum* in the center of its track (□), in the ridge at the margin of its track (●), and in adjacent, undisturbed sediment (○). Dashed lines indicate position of the sediment surface

contrast, the diffusivities of the sediment along the center of the track did not differ from those of undisturbed sediment. Aquaria containing echinoids had a luxuriant growth of algae and cyanobacteria on submerged surfaces, whereas no such growth was evident in similar aquaria without echinoids.

Echinoid respiration

Echinocardium cordatum consumed 356.2 ± 183.6 nmol O_2 h^{-1} (116.8 ± 48.4 nmol O_2 g dry wt^{-1} h^{-1}). The length, width, and height of specimens were 40.0 ± 2.5, 36.1 ± 1.7, and 28.3 ± 2.9 mm, respectively. Body volume was 10.9 ± 2.1 cm^3, and wet and dry weights were 11.5 ± 2.1 and 3.0 ± 0.6 g, respectively.

DISCUSSION

We studied for the first time *in situ* [O_2] around burrowing echinoids at sub-millimeter resolution under different flow conditions. Our measurements revealed steep [O_2] gradients in the sediment surrounding burrowing echinoids under conditions of calm weather and steady, near-bottom flow. [O_2] maxima at the surface of sediment that had not been disturbed by *Echinocardium cordatum* for some time, associated pH maxima, and deep penetration of O_2 (Fig. 3) resulted from benthic photosynthesis. That is, during daytime, the near-bottom seawater and pore water were supplied with O_2 from photosynthetic production at the sediment surface. Flow over elevated sediment can cause pore-water advection (Huettel & Gust 1992), which will remove such O_2 peaks. However, the absence of [O_2] maxima in the elevated sediment above burrowing *E. cordatum* may not be a consequence of increased transport, but rather of the disturbance of the microphyte community by its feeding and its displacement of sediment. This effect seems to be confined to the sediment above each echinoid, because O_2 profiles measured behind echinoids resembled those in the surrounding sediment.

The large standard deviations of average [O_2] in undisturbed sediment shown in Fig. 3b were probably caused by patchy distribution of benthic phototrophs, which was also indicated by patchy coloration of the sediment surface. We infer that disturbance of the sediment by *Echinocardium cordatum* removes this patchiness, because sediment properties in the tracks immediately behind the echinoid were more homogeneous than those immediately in front. Given that 33 ind. m^{-2} (70% of 47 ind. m^{-2}) rework the sediment at a speed of ~2 cm h^{-1}, and that the width of their tracks is 3.4 cm, we calculated that *E. cordatum* reworks ~224 cm^2 seafloor h^{-1}, implying that it reworks the seafloor every 45 h. That is, patchiness in the distribution of benthic phototrophs may be a result of a rapid succession following disturbance. After the passage of *E. cordatum*, a surface community of phototrophic organisms may have re-established within a few hours by horizontal migration (see Consalvey et al. [2004] for a review). Some diatom species can move horizontally at speeds up to 3.2 cm h^{-1} (Happey-Wood & Jones 1988), matching the maximum speed recorded for *E. cordatum* in this study, and the re-establishment of phototrophic communities may be advanced by favorable nutrient supply from the freshly reworked sediment. That is, a population of shallow-burrowing *E. cordatum* turns a consolidated, smooth, greenish-brown sediment–seawater interface (observed at other sites of Mahurangi Harbour not populated by *E. cordatum*) into a mosaic of sediment patches whose surfaces differ in

coloration, diffusive properties (Figs. 1a & 5b), and time of exposure to E_d(PAR) and oxygenated bottom seawater. Owing to the smoothing effect of molecular diffusion (Røy et al. 2005), the smaller-scale biologically produced topography may have only marginally increased the size of the 3-dimensional surface for the diffusive exchange of O_2 (<12% increase). The effect of *E. cordatum* on the area of this exchange surface appears to be more pronounced. Also, enhanced bed roughness and a possible 'loosening' of the uppermost sediment due to frequent reworking may increase bed shear stress and reduce the critical erosion shear stress, respectively, and thus increase the likelihood for sediment resuspension.

The relatively low [O_2] measured at the front funnel indicated that *Echinocardium cordatum* pumped seawater from the surface of the sediment into the intrafasciolar region through the rear funnel, over the respiratory tube feet (where O_2 was extracted), and around the outer surface of the test, finally returning it to the surface of the sediment via the front funnel. Foster-Smith (1978) presented evidence that *Echinocardium* spp. can generate higher pressures than other animals with ciliary pumps; however, at our study site, *E. cordatum*'s 2 large funnels made a build-up of pressure around the test unlikely, and percolation of seawater was not indicated by any of the [O_2] profiles measured behind buried *E. cordatum*. Under conditions of steady, near-bottom flow, the supply of O_2 to the sediment immediately surrounding *E. cordatum* is a function of (among other factors) the oxygenation of the respiratory current, which is affected by O_2 production and consumption at the sediment surface and the echinoid's respiration. For example, the respiratory current can be O_2-supersaturated during daylight. Assuming that the O_2 gradients in the sediment surrounding the apical region of *E. cordatum* were in steady state and were representative of the entire animal–sediment interface (~5.9×10^{-3} m^2), and that this interface was flat, we calculated that the O_2 flux from the respiratory current of an individual echinoid into the surrounding sediment would be ~860 nmol h^{-1}—at least twice the respiration rate of the echinoid (Vopel et al. [2003] found a similar ratio for the brittle star *Amphiura filiformis*). If the total O_2 demand caused by a buried, moving *E. cordatum* (echinoid respiration plus sediment demand) was 1.2 µmol h^{-1}, the seawater pumped around the outer surface of the test was returned to the sediment surface via the frontal funnel, and [O_2] in the intrafasciolar region was 10% higher than that at the opening of the front funnel, then the pumping rate would be 51 cm^3 h^{-1}. This rate is within the known range of *Echinocardium* spp. in sand (40 to 135 cm^3 h^{-1}, mean 90 cm^3 h^{-1}, Foster-Smith 1978). The cross-sectional area of an average-sized adult individual (length with spines = 4 cm) was ~12 cm^2 (see Lohrer et al. [2005] for relationship between length and cross-sectional area). If such an individual progressed through the sediment at 1 to 3 cm h^{-1}, it would displace only 12 to 36 cm^3 sediment h^{-1}; therefore, *E. cordatum* pumps a greater volume of seawater than it displaces of sediment per unit time.

Although *Echinocardium cordatum* generates heterogeneity with respect to the horizontal distribution and activity of phototrophic organisms and pore-water [O_2] at the sediment–seawater interface, it mixes particles and thus may homogenize the distribution of slowly reacting dissolved and solid-phase chemical species in deeper sediment. By simultaneously mixing and irrigating the sediment, heart urchins may regenerate and introduce solid-phase oxidants into the upper sediment column, thereby modifying the relative importance and depth distribution of redox-reaction pathways and consequently the production and consumption of protons. Our measurements in the upper 5 mm of undisturbed and track sediment revealed an increase in pH to a subsurface peak, followed by a steep decrease to a local minimum below the oxic zone (Fig. 5). We attributed the shape of these profiles to carbonic acid consumption and production by photosynthesis and oxic respiration, respectively, and the oxidation of reduced inorganic species (Van Cappellen & Wang 1996, Jourabchi et al. 2005). The observed trend of increasing pH with depth in the deeper suboxic zone of the track sediment may result from reductive dissolution of regenerated solid phase-oxidants such as iron and manganese (hydr)oxides.

We demonstrated that the zone of oxic sediment around *Echinocardium cordatum* is narrow (Fig. 4, Table 2), as is the path for the diffusion of reduced metabolites from the sediment into the seawater surrounding the echinoid. Increased release of reduced metabolites from the sediment around *E. cordatum* was also indicated by our observation of luxuriant growth of phototrophs on submerged surfaces in aquaria containing echinoids, and by the observations of Lohrer et al. (2004) that the concentrations of ammoniacal nitrogen in the seawater of benthic chambers is positively correlated with the density of enclosed echinoids. In the field, solute exchange across the interface between the seawater and sediment surrounding *E. cordatum* may be further increased as a result of wave action (Riedl et al. 1972, Webster 2003). We did not measure time series of [O_2] in the pore water of sediment immediately surrounding *E. cordatum*, but our measurements in nearby undisturbed sediment indicated that wind waves induced oscillating pore-water motion at depths of at least 10 mm. Following Webster & Tayler (1992) and Webster (2003), we suggest that the observed oscillations in motions of both sediment

pore water and seawater around the test of *E. cordatum* (Fig. 2f) lead to enhanced diffusivities through the mechanism of shear dispersion, and thereby increase the sediment–seawater solute exchange across both the sediment surface and the sediment–seawater contact zone around *E. cordatum*.

Because *Echinocardium cordatum* increases the topography of the sediment surface at our study site, increased exchange of O_2 may also be observed under conditions of calm weather and steady bottom flow. We detected higher apparent diffusivity in the uppermost layer of raised sediment flanking the depression along the path of *E. cordatum* in aquaria (Figs. 1a & 5a), and we speculated that flows over this sediment can increase solute exchange. Data presented by Lohrer et al. (2004) support this speculation. They observed that during darkness, the O_2 demand of flowing seawater in benthic chambers increased with the density of burrowing *E. cordatum* (p. 1093, their Fig. 3a). The individual contribution to changes in chamber O_2 demand calculated from the slope of the partial-regression residual plot in Lohrer et al.'s (2004) Fig. 3a was -6.94 µmol O_2 m^{-2} h^{-1} (A. M. Lohrer pers. comm.) If the total O_2 demand of a burrowing *E. cordatum* was 1.2 µmol h^{-1} (see above), then more than 80% of the individual contribution may have resulted from processes other than respiration and irrigation; one possibility would be a gradual increase in the flux of solutes such as O_2 caused by flow over the surface of a sediment that became increasingly rough and porous as the density of *E. cordatum* increased. This effect may not only explain the steep increase in the O_2 demand of chambers with increasing numbers of added *E. cordatum* under conditions of darkness, but also the observed opposite effect under conditions of daylight (Figs. 2d,f & 3b in Lohrer et al. 2004).

Acknowledgements. G. Funnell assisted in the field. V. Cummings, A. M. Lohrer, S. Nodder, and A. B. Thistle commented on an earlier version of the manuscript. We are grateful for the constructive criticism of 4 anonymous reviewers. The New Zealand Foundation for Research, Science and Technology (C01X0212) funded our research.

LITERATURE CITED

Berg P, Risgaard-Petersen N, Rysgaard S (1998) Interpretation of measured concentration profiles in sediment pore water. Limnol Oceanogr 43:1500–1510

Bird FL, Ford PW, Hancock GJ (1999) Effect of burrowing macrobenthos on the flux of dissolved substances across the water–sediment interface. Mar Freshw Res 50: 523–532

Broecker WS, Peng TH (1974) Gas exchange rates between air and sea. Tellus 26:185–190

Buchanan JB (1966) The biology of *Echinocardium cordatum* (Echinodermata: Spatangoidea) from different habitats. J Mar Biol Assoc UK 46:97–114

Consalvey M, Paterson DM, Underwood GJC (2004) The ups and downs of life in a benthic biofilm: migration of benthic diatoms. Diatom Res 19:181–202

De Ridder C, Jangoux M, De Vos L (1987) Frontal ambulacral and peribuccal areas of the spatangoid echinoid *Echinocardium cordatum* (Echinodermata): a functional entity in feeding mechanism. Mar Biol 94:613–624

Fenchel T, Glud RN (2000) Benthic primary production and O_2-CO_2 dynamics in a shallow-water sediment: spatial and temporal heterogeneity. Ophelia 53:159–171

Foster-Smith RL (1978) An analysis of water flow in tube-living animals. J Exp Mar Biol Ecol 34:73–95

Giere O (1993) Meiobenthology: the microscopic fauna in aquatic sediments. Springer-Verlag, Berlin

Happey-Wood CM, Jones P (1988) Rhythms of vertical migration and motility in intertidal benthic diatoms with particular reference to *Pleurosigma angulatum*. Diatom Res 3: 83–93

Hollertz K, Duchêne JC (2001) Burrowing behaviour and sediment reworking in the heart urchin *Brissopsis lyrifera* Forbes (Spatangoida). Mar Biol 139:951–957

Huettel M, Gust G (1992) Impact of bioroughness on interfacial solute exchange in permeable sediments. Mar Ecol Prog Ser 89:253–267

Huettel M, Webster IT (2000) Porewater flow in permeable sediment. In: Boudreau BP, Jørgensen BB (eds) The benthic boundary layer: transport processes and biogeochemistry. Oxford University Press, Oxford, p 144–179

Jourabchi P, Van Cappellen P, Regnier P (2005) Quantitative interpretation of pH distributions in aquatic sediments: a reaction-transport modeling approach. Am J Sci 305: 919–956

Kanazawa KI (1995) How spatangoids produce their traces: relationship between burrowing mechanisms and trace structure. Lethaia 28:211–219

Li YH, Gregory S (1974) Diffusion of ions in sea water and in deep-sea sediments. Geochim Cosmochim Acta 38: 703–714

Lohrer AM, Thrush SF, Gibbs MM (2004) Bioturbators enhance ecosystem function through complex biogeochemical interactions. Nature 431:1092–1095

Lohrer AM, Thrush SF, Hunt L, Hancock N, Lundquist C (2005) Rapid reworking of subtidal sediments by burrowing spatangoid urchins. J Exp Mar Biol Ecol 321: 155–169

Nichols D (1959) Changes in the chalk heart-urchin *Micraster* interpreted in relation to living forms. Phil Trans R Soc Lond Ser B 242:347–437

Osinga R, Lewis WE, Wopereis JLM, Vriezen C, Van Duyl FC (1995) Effects of the sea urchin *Echinocardium cordatum* on oxygen uptake and sulphate reduction in experimental benthic systems under increasing organic loading. Ophelia 41:221–236

Rasmussen H, Jørgensen BB (1992) Microelectrode studies of seasonal oxygen uptake in a coastal sediment: role of molecular diffusion. Mar Ecol Prog Ser 81:289–303

Revsbech NP (1989) An oxygen microelectrode with a guard cathode. Limnol Oceanogr 34:474–478

Revsbech NP, Nielsen LP, Ramsing NB (1998) A novel microsensor for determination of apparent diffusivity in sediments. Limnol Oceanogr 43:986–992

Riedl R, Huang N, Machan R (1972) The subtidal pump: a mechanism of intertidal water exchange by wave action. Mar Biol 13:210–221

Røy H, Huettel M, Jørgensen BB (2005) The influence of topography on the functional exchange surface of marine

soft sediments, assessed from sediment topography measured *in situ*. Limnol Oceanogr 50:106–112

Ullman WJ, Aller RC (1982) Diffusion coefficients in nearshore marine sediments. Limnol Oceanogr 27: 552–556

Van Cappellen P, Wang Y (1996) Cycling of iron and manganese in surface sediments: a general theory for the coupled transport and reaction of carbon, oxygen, nitrogen, sulfur, iron and manganese. Am J Sci 296:197–243

Vopel K, Thistle D, Rosenberg R (2003) Effect of the brittle star *Amphiura filiformis* (Amphiuridae, Echinodermata) on oxygen flux into the sediment. Limnol Oceanogr 48: 2034–2045

Webster IT (2003) Wave enhancement of diffusivities within surficial sediments. Environ Fluid Mech 3:269–288

Webster IT, Tayler JH (1992) Rotational dispersion in porous media due to fluctuating flow. Water Resour Res 28: 109–119

Editorial responsibility: Howard Browman (Associate Editor-in-Chief), Storebø, Norway

Submitted: March 27, 2006; Accepted: August 12, 2006
Proofs received from author(s): March 1, 2007